# Calcium phosphate coated core-shell protein nanocarriers: robust stability, controlled release and enhanced anticancer activity for curcumin delivery

by Wu, Q., Gao, H., Vriesekoop, F., Liu, Z., He, J. and Liang, H.



DOI: https://doi.org/10.1016/j.msec.2020.111094


Wu, Q., Gao, H., Vriesekoop, F., Liu, Z., He, J. and Liang, H. 2020. Calcium phosphate coated core-shell protein nanocarriers: robust stability, controlled release and enhanced anticancer activity for curcumin delivery. *Materials Science and Engineering: C*.
19 May 2020

## Highlights

- NaCas@CaP nanodelivery system has nano-size and core-shell structure.
- The mechanism of encapsulation was characterized and analyzed.
- The stability of the encapsulated Cur was significantly improved.
- The pH-responsive release around the cancer cell was achieved.
- The encapsulated Cur existed better cellular anti-oxidant and anti-cancer ability.

# Calcium Phosphate Coated Core-Shell Protein Nanocarriers: Robust Stability, Controlled Release and Enhanced Anticancer Activity for Curcumin Delivery

Qiao Wu[a] Huiling Gao[a] Frank Vriesekoop[c] Zexun Liu[a] Jie He[a] Hao Liang*[a b]

[a] State Key Laboratory of Chemical Resource Engineering, Beijing University of Chemical Technology, Beijing100029, P.R. China

[b] Qinhuangdao Bohai Biological Research Institute of Beijing University of Chemical Technology, Qinhuangdao 066000, China

[c] Department of Food Technology and Innovation, Harper Adams University, Newport TFl0 8NB, Shropshire, United Kingdom

Corresponding Author

* E-mail: lianghao@rnail.buct.edu.cn

ABSTRACT: Composite protein and inorganic nanodelivery systems can realise a pH-responsive release and effectively improve the stability and anti-cancer proliferative activity of hydrophobic molecules. In this study, a novel core-shell

structure of NaCas (Sodium Caseinate)@CaP (Calcium Phosphate) as a nanodelivery system with NaCas as the core for increasing solubility and CaP as the shell for enhanced stability was built. By using Cur (Curcumin) as a model bioactive molecule, (Cur@NaCas)@CaP nanoparticles (NPs) demonstrated a uniform size distribution of 150-200 nm with a distinct nano-composite structure. After exposure to 80 °C for 2 h, the NaCas@CaP loaded Cur still retained 80% stability while under the same conditions only 12 % of free Cur remained intact. UV-light stability was remarkably enhanced 8.56 fold by the protection of the core-shell structure. More importantly, pH-responsive release was achieved owing to the CaP surface coating. The encapsulated Cur by NaCas@CaP NPs exhibited an enhanced cellular anti-oxidant activity (CAA) based on MGC-803 cell monolayer models. The confocal laser-scanning microscopy (CLSM) images and cancer-cell-proliferation assay illustrated that (Cur@NaCas)@CaP NPs showed significantly improvements of cellular uptake and anti-cancer activity against A549 cancer cells than free Cur. These novel core-shell NaCas@CaP NPs are very promising for intensifying the stability and bioactivity of hydrophobic compounds in drug delivery and cancer treatment.

***Key words:*** Nanodelivery, Sodium caseinate, Calcium phosphate, Curcumin, Anti-oxidant, Anti-cancer

## 1.Introduction

Natural self-assembled delivery systems are nanodelivery systems formed by the self-assembly of natural biomaterials with nanostructures.[1, 2] These biomaterials can spontaneously form regular shapes, such as spheres, cylinders, lamellae, etc., by relatively weak non-covalent interactions at concentrations well above their critical micelle concentration.[3-5] These systems are mainly used to encapsulate, protect and transport functional active substances because of their enhanced permeability and retention effect.[6, 7] The enhanced permeability and retention effect refers to the notion that certain macromolecules and nanoparticles accumulate inside tumor tissues at greater concentrations compared to non-tumor tissues.[8] Compared with traditional embedding technologies, natural self-assembled delivery systems have size-related effects, due to the relatively random nature of the self-assembly process which results in a heterogeneous range of surfaces and sized particles. Furthermore, natural self-assembled delivery systems also have different in vivo distribution specificity with regards to the targeted delivery of drugs and nutritional compounds.[9, 10] Moreover, biodegradable self-assembled delivery systems improve the bioavailability of guest molecules, and can achieve a controlled and sustained release, and facilitate targeted delivery of bioactive compounds.[11] Due to their biodegradability, natural self-assembled delivery systems pose minimal cytotoxicity, are renewable and have an abundant availability, a high drug binding capacity, and a significant uptake by target cells, protein-based delivery systems, including zein,[11] soy protein isolate,[12] sodium caseinate[13] and ferritins,[14] have received increasing attention as natural self-assembled delivery systems.

Sodium caseinates (NaCas) is a widely used food additive derived from milk. With distinct hydrophobic and hydrophilic domains, NaCas can self-assemble into a stable micellar structure in aqueous solution, especially when its concentration is higher than the its critical micelle concentration.[13] Due to its excellent biocompatibility and biodegradability, and limited immunogenicity, NaCas is regularly employed as a unique natural self-assembled nanodelivery material in biological applications.[15] NaCas has been used to enhance the solubility, stability and bioavailability of otherwise insoluble natural compounds, especially those with considerable biological activity, such as some vitamins and their precursors, [16-18] and antioxidants.[19]

Although the deployment of NaCas is a strategic improvement in the delivery of otherwise recalcitrantly soluble bioactive molecules, the long-term stability of NaCas nanoparticles (NPs) remains a major obstacle for their successful applications as delivery vehicles. The structural integrity of NaCas is readily compromised as a consequence of changes in pH, ionic strength, water activity, temperature or pressure,[20] which causes an imbalance between hydrophobic and electrostatic interactions.[21, 22] Various strategies for improving the stability of NaCas nanostructures are emerging. Organic materials such as pectin,[23] chitosan,[24] alginates,[25] and combinations thereof [26] have been used to stabilize NaCas NPs. However, even these nanocarriers still fall short of providing sufficient physicochemical stability and often require complicated assembly processes.[27, 28] Therefore, a stable nanoscale NaCas system with a simple assembly method for its synthesis is urgently needed for the delivery of sensitive molecules.

Hybridization of organic and inorganic carriers can confer nanomaterials with new stability related properties not normally associated with the individual carriers.[29, 30] Calcium phosphate (CaP) NPs have good adsorption capacity and pH-responsive release characterization for both proteins and drugs.[31-33] CaP NPs can deliver diagnostic and therapeutic agents with minimal toxicity for the detection and treatment of various diseases including cancer.[34]In order to improve the stability of NaCas particles, we chose CaP to provide a secondary coating and as such address the premature release from compounds encapsulated by NaCas.[13] We constructed hybrid NaCas-CaP NPs (NaCas@CaP NPs) with a stable core-shell structure by means of a simple, one-pot method under mild conditions using curcumin (Cur), a natural anti-cancer biomolecule, as a model guest molecule **(Scheme 1).** Cur was encapsulated into the core of NaCas micellar particles by hydrophobic interactions during the self-assembly process of dissociated NaCas, yielding Cur@NaCas NPs. The Cur@NaCas surface was simultaneously coated with CaP as a stable shell. The formation and conformation of the encapsulated-core-and-shell NPs were characterized by various means. The stability and *in vitro* releasing of (Cur@NaCas)@CaP NPs at physiological pH and the pH encountered in cancer cells were examined. In addition, the cellular uptake ability, the cellular anti-oxidant activity and in vitro cell proliferation assay of the inclusion complexes were tested and compared with free Cur. Our results indicated that the NaCas@CaP NPs with high efficiency and stability are a novel nanoplatform for cancer therapy and free

radical scavenging *in vivo*. Furthermore , the NPs have universality for hydrophobic sensitive molecules, which make these NPs a promising drug delivery system.

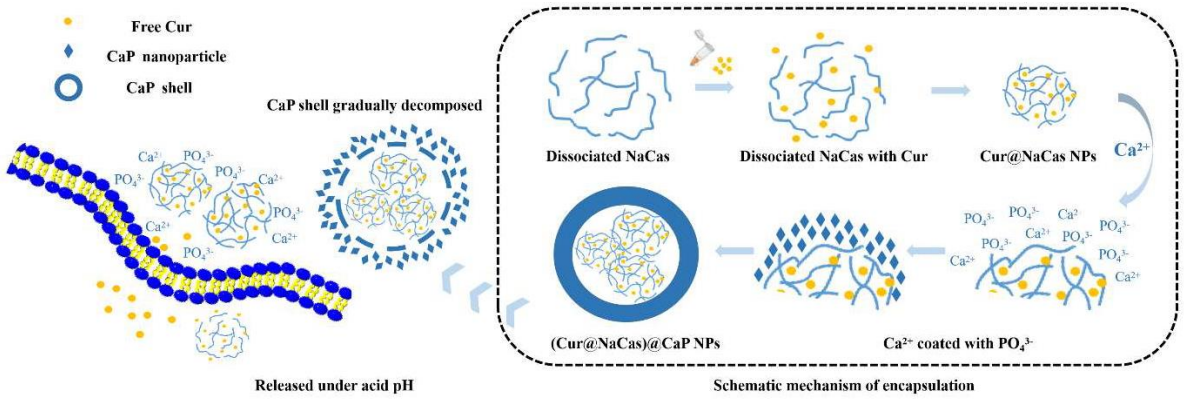


**Scheme 1** Schematic mechanism of encapsulation and cell-uptake of NaCas@CaP loaded Cur.

## 2 Material and methods

### 2.1 Materials and Cell Culture

Curcumin (Cur, 98 %), sodium caseinate (NaCas) were purchased from Macklin Biochemical Co., Ltd, (Shanghai, China). 2,2-azobis (2-amidinopropane) dihydrochloride (ABAP), 2,7-dichlorodi-hydrofluorescein diacetate (DCFH-DA), and Propidium Iodide (PI) were obtained from Sigma-Aldrich, (St Louis, MO, USA). Cell Counting Kit-8 (CCK-8) was obtained from Dojindo Laboratories (Tokyo, Japan). All other chemicals (analytical grade) were purchased from Beijing Chemical Works (Beijing, China), and were applied without further purification. Human gastric cancer cells (MGC803) and human alveolar basal epithelial cancer cells (A549 cells) were obtained from the Cell Resource Center, Peking Union Medical College (Beijing,

China), and cultured with DMEM supplemented with 10 % Fetal Bovine Serum and 1 % P/S at 95+% RH with 5 % $CO_2$ at 37 °C.

## 2.2 Preparation of (Cur@NaCas)@CaP NPs

Samples were prepared by rehydrating NaCas in 10 mM phosphate buffer solution (pH 7.4) at room temperature (25 °C) with moderate stirring for 30 min to produce a NaCas stock solution at 1 mg/mL. A Cur stock solution of 500 μg/mL in absolute ethyl alcohol was prepared. 200 μL of the Cur stock solution was vigorously mixed at 600 rpm with 1 mL NaCas solution at room temperature for 2 h. The successfully encapsulated Cur (Cur@NaCas) was separated from the non-encapsulated Cur by centrifugation at 290 g for 10 min. The resultant supernatant containing the Cur@NaCas was subjected to (i) secondary encapsulation, (ii) particle property characterization or (iii) freeze-drying to produce Cur@NaCas NPs for further study.

Un-encapsulated Cur on the bottom was measured in order to calculate the drug loading efficiency (DLE). Free curcumin was determined by UV-vis at 428 nm. The DLE of Cur@NaCas was calculated according to following eq.(1):

$$DLE(\%) = \frac{\text{total amount of added Cur - amount of Cur on the bottom}}{\text{total amount of added Cur}} \times 100\% \quad (1)$$

To facilitate the secondary encapsulation, 20 μL calcium chloride (CaCb) solution (50 mM) was added to the Cur@NaCas NPs solution in PBS (10 mM, pH 7.4) to form (Cur@NaCas)@CaP NPs. The mixture was mixed using a vortex mixer (SCILOGEX MX-S) for 2 min and then allowed to stand for 24 h. The precipitate was either used for immediate particle property characterization or it was freeze-dried to produce the

(Cur@NaCas)@CaP NPs powders that were used for further study. Un-encapsulated Cur@NaCas on the supernatant was measured in order to calculate the DLE. The DLE of (Cur@NaCas)@CaP was calculated according to following eq.(2).

$$(2)\ \mathrm{DLE} = \frac{\text{total amount of added Cur@NaCas - amount of Cur@NaCas in supernatant}}{\text{total amount of added Cur@NaCas}} \times 10001_{,0}$$

## 2.3 Characterization

The various samples used and constructed in this study (NaCas, Cur@NaCas and (Cur@NaCas)@CaP) were investigated using transmission emission microscopy (TEM, Hitachi HT7700, Tokyo, Japan) and scanning electron microscope (SEM, Hitachi S-4700, Tokyo, Japan).[35] The average size and zeta-potential of free Cur and the various inclusion complexes were ascertained using dynamic light scattering (DLS, Nano-ZS 2000, Malvern Instruments, UK). The crystalline characterization of free Cur and the various inclusion complexes was facilitated using X-ray diffractometer (XRD, D8 ADVANCE, Germany, Bruker) at a diffraction angle of 20 ranging from 5° to 50° with a stepwise scan rate of 10°/min at 0.2° per step. The FT-IR spectra of freeze-dried samples were obtained using a fourier-transform infrared spectrometer (FT-IR, Nicolet 6700, Madison, WI, USA) with a scanning range of 4000 - 500 cm-·[1] The fluorescence spectra for free Cur and encapsulated Cur were recorded by employing a fluorescence spectrophotometer (Hitachi F7000, Tokyo, Japan) at an excitation wavelength of 420 nm, with the emission spectra being recorded of a range from 440 - 650 nm at a slit width of 5 nm. Dispersions of inclusion complexes were prepared in deionized water. Free Cur was dissolved in ethanol or deionized water to the same final concentration as in the encapsulated Cur.

## 2.4 *In vitro* stability of nano-encapsulated Cur

The *in vitro* stability of free Cur and the various NPs was determined according to a previously reported method.[12] Following the various treatments, the samples were

centrifuged and the ethanolic supernatant was analyzed by HPLC(Liquid column: $C_{18}$ (200 mmx 4.6 mm, 5μm); Mobile phase: 0.1% phosphate - acetonitrile (50:50); Detection wavelength: 430 nm; Velocity of flow: 1.0 ml/min ; 25°C; Injection volume: 20 μL). The initial data for all the cases was set as 100%.

### 2.5 *In vitro* release of Cur

The *in vitro* release of Cur from NaCas or NaCas@CaP NPs was established by a dialysis protocol according to a method reported elsewhere.[36] First, Cur loaded inclusion complex were fully dispersed in a release medium (PBS, pH 7.4 or pH 5.5) in a dialysis bag (MWCO 3500Da), which was then put into a dissolution apparatus, and immersed in 200 mL of the dissolution medium with 1 ¾(w/v) Tween-80 under gentle stirring at a rate of 100 rpm at 37 °C. At various time intervals, an aliquot of the sample was extracted and analyzed to determine the release of Cur by HPLC.

### 2.6 Cellular Uptake Measured by Confocal Laser Scanning Microscope.

A549 cells ($4x10^4$ cells/well) were attached to a confocal laser dish over a 12 h period, after which the cells were washed once with PBS and treated with either free Cur or Cur-loaded NPs (2 mL, 5 μg/mL, in DMEM) and incubated at 37 °C, 5 % $CO_2$ for 6 h. Then the cells were washed twice with PBS to remove all extracellular Cur. A 4 % paraformaldehyde solution was added to fix the cells (at room temperature for 30 min), after which 200 μL PI was added to stain the cell nucleus for 15 min. Prior to imaging , all the cells samples were washed once more with PBS. The images of confocal laser scanning microscope (CLSM) were captured by exciting Cur at 442

run, PI at 488 run, with emissions measured at 475 run and 630 run respectively.

### 2.7 Cellular Antioxidant Activity

Cellular antioxidant activity (CAA)was determined according to the method reported previously.[35]Briefly, MGC803 cells were seeded in 96-well plates with a concentration of $2.5 \times 10^5$ cells per milliliter and incubated for 24 h. Then the growth medium was removed and replaced with either 100 µL fresh medium containing 2 µg/mL free Cur or Cur-loaded NPs and incubated for another 24 h. After 24h, fresh medium (100 µL) containing 25 µM DCFH-DA was added into each well and incubated for 1 h. Then, all wells were rinsed with PBS before 100 µL fresh medium containing 600 µM ABAP was added into each well. A microplate reader employing an excitation wavelength of 485 run and an emission wavelength of 535 run was used to measure the fluorescent intensity of samples, over an 1 h period at 5 minutes intervals. The control samples were treated with DCFH-DA and ABAP only, while the blank samples contained cells treated with DCFH-DA only. The area under the time-fluorescence intensity curve can be obtained by integration, and the antioxidant activity (CAA) units for natural antioxidant can be calculated using the following eq.(3):

$$(3)\ CAA = 100 - (f_{SA}/f_{CA}) \times 100$$

$f_{SA}$ represent the integral area of the fluorescence value-time curve by adding different concentrations of Cur;

$f_{CA}$ represent the integral area of the blank group fluorescence value-time curve.

### 2.8 In Vitro Cell Anti - proliferation Assay.

A549 cells were seeded into 96-well microtiter plates at a density of 4000 cells per well in 100 µL of medium. After 24 h, the cells were treated with a medium containing DMSO-dissolved Cur, NaCas-encapsulated or NaCas@CaP-encapsulated Cur. Other cells were untreated (negative controls) or treated only with DMSO, NaCas or NaCas@CaP NPs at the concentrations as in the dispersions with encapsulated curcumin (positive controls). After 72 h treatmen,t CCK-8 solution (20 µL) was added to each well and then incubated for 1 h. The absorbance at 450 nm was measured with a microplate reader (Bio-Tek Instruments, Winooski , VT). The normalized cell viability was obtained after normalizing the viability of a treatment by the viability of control cells treated with DMSO only. The cell viability can be calculated using the following eq.(4):

$$\text{Cell viability} = \left(A_{treated}/A_{control}\right) \times 100\% \quad (4)$$

where $A_{treated}$ and $A_{control}$ are the absorbance of the wells with cells treated by Cur and the control, respectively. The mean and standard deviation from three-well replicates were calculated.

## 3. Results and discussion

### 3.1 Preparation and Characterization of CaP coated Core-Shell nanoparticles

(Cur@NaCas)@CaP NPs were prepared using the self-assembly and surface-coating method outlined above. By adjusting the concentration of NaCas and the stirring speed during the encapsulation access, the optimized conditions were

233 determined as: l mg/mL NaCas **(Table S1),** 600 rpm/min **(Table S2),** 2h **(Table S3),**
234 achieving a DLE of 90.01±1.29 %. See the supplementary data for more in-depth data
235 about the optimization of this methodology.

236 After that, calcium ions as CaCh were added which interacted with the phosphate
237 in PBS, which in tum allowed the formation of a CaP coating on the surface ofNaCas
238 protein to obtain Cur@NaCas)@CaP. The DLE of (Cur@NaCas)@CaP under
239 optimized conditions of CaP **(Table S4)** was 99.25±1.97 %.

240 TEM was performed to identify the formation of core-shell structure, and the size
241 distribution of particles was determined by DLS **(Figure lG).** The native NaCas
242 appeared as uniform and compact spherical structure **(Figure lA)** with an average
243 size of 28 nm. The particle size of Cur@NaCas NPs was slightly larger than that of
244 native NaCas **(Figure 1B)** with an average size of 32 nm. After the application of a
245 $Ca3(PO_4)_2$ coating, the formed particles in the range of 195-205 nm, with the TEM
246 image **(Figure 1**C) revealing a clear core-shell structure. The TEM image shows that
247 the core size of the hybrid NPs ranged from 80 to 120 nm, which is probably due to
248 the aggregation of Cur@NaCas. SEM also demonstrated the dimension change of
249 NPs and the results **(Figure 1D-F)** consistent with the TEM images.

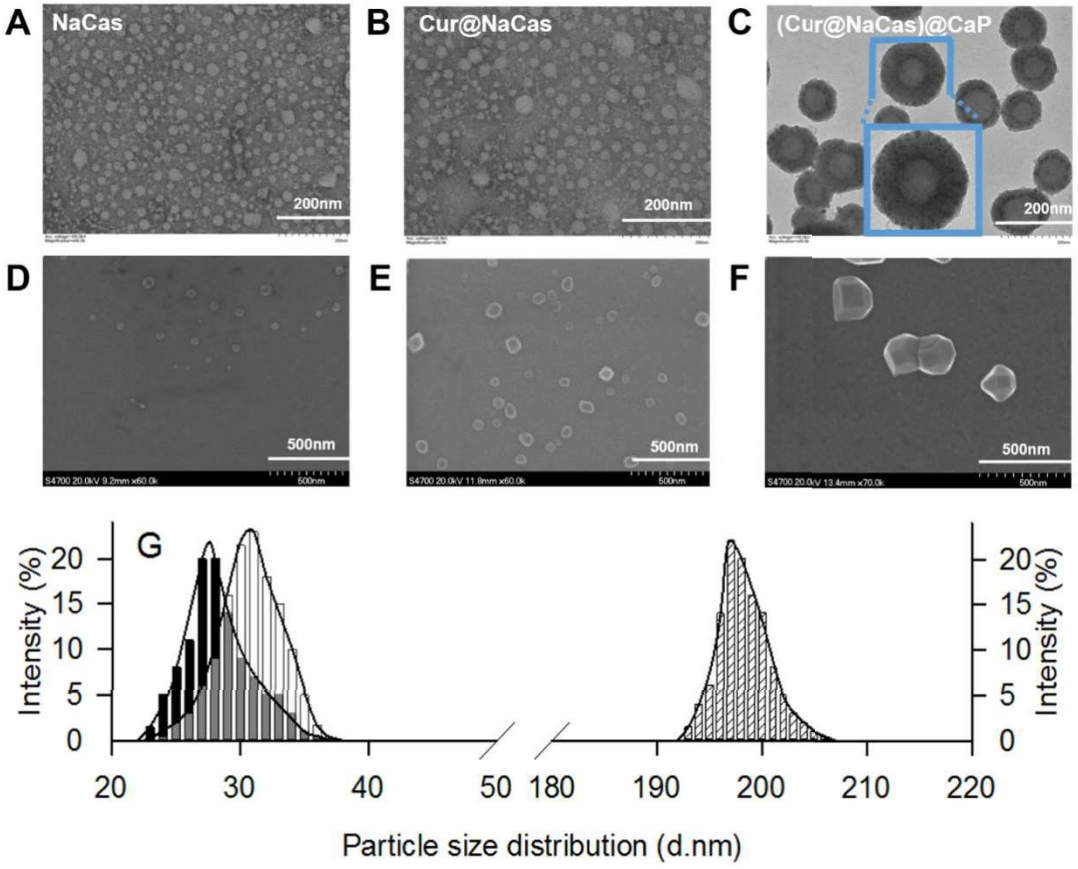


250

251 **Figure 1.** Transmission electron microscopy (TEM) (A, B, and C) and scannmg
252 electron microscopy (D, E, and F) and particle size distribution of native NaCas (A,
253 D, G), Cur@NaCas NPs (B, E, G) and (Cur@NaCas)@CaP NPs (C, F, G). G
254 represent the particle size distribution of: native NaCas (black bars ranging from 22 to
255 38 nm); Cur@NaCas (white bars ranging from 22 to 38 nm) the grey bars (24 to 36
256 nm) represent the overlapping particle size distribution between native NaCas and
257 Cur-in-NaCas ; and (Cur@NaCas)@CaP respectively (hatched bars ranging from 192
258 to 208 nm). The blue boxed area in (C) shows a high magnification of this region by
259 TEM.

260

261 The formation of the CaP shell was further evidenced by XRD. The XRD patterns

for free Cur (a), NaCas (b), Cur@NaCas NPs (c), (Cur@NaCas)@CaP NPs (d) and NaCas@CaP NPs (e) are shown in **Figure 2A.** The powder diffraction pattern of Cur displayed several sharp peaks at diffraction angles of 8, 8.9, 14.5, 17.2, 21.1, suggesting that Cur existed in a crystalline form.[35, 37] Although NaCas was amorphous lacking crystalline peaks (line ' b'), some minor evidence of crystalline forms persisted in the Cur@NaCas NPs (line ' c' ). The minor crystalline signals might be due to fractions of the entrapped Cur protruding from the NaCas casing, which is likely to be the result of the spontaneous encapsulation of free Cur by NaCas. Furthermore , the characteristic peak of (Cur@NaCas)@CaP NPs and NaCas@CaP NPs showed the same position with the complete absence of any diffraction peak corresponding to Cur, indicating the formation of (Cur@NaCas)@CaP NPs where the NaCas@CaP core-shell formation completely shielded the encapsulated Cur.

FT-IR spectroscopy was performed to verify the interaction between NPs and Cur, and also to confirm the mechanisms of encapsulation and surface coating. The FT-IR spectra of free Cur (a), NaCas (b), Cur@NaCas NPs (c), (Cur@NaCas)@CaP NPs (d) and NaCas@CaP NPs (e) are shown in **Figure 2B.** Cur was characterized by discrete absorption peaks at 3502 cm-I (phenolic O-H stretching,) 1720 cm-I (C=O stretching on the diketone groups), 1614 $cm^{-1}$ and 1000 $cm^{-1}$ (C=C bending on the aromatic rings), 1515 $cm^{-1}$ (C=C stretching in aromatic ring), 1450 $cm^{-1}$ (C-H bending on methyl groups), and 1300-1200 $cm^{-1}$ (=C-O-$CH_3$ stretching of alkyl-aryl ether groups). Most of the characteristic peak of Cur disappeared after encapsulation by NaCas.[38] For NaCas, the characteristic peaks of at 3424 $cm^{-1}$ (free O-H, N-H

absorbing), 1644 (amide I group) shifted to 3415 cm-$^{1}$, 1628 cm-$^{1}$ respectively after self-assembling with Cur. These shifts are most likely due to the notion that hydrogen bonds of NaCas participated in the formation of Cur@NaCas NPs, which involved changes in the secondary structure of NaCas proteins.l$^{39}$1 Furthermore, the peaks of (Cur@NaCas)@CaP NPs at 1123 cm-$^{1}$, 1027 cm-$^{1}$, 599 cm-$^{1}$ and 559 cm-$^{1}$ remained the same as NaCas@CaP NPs, which appeared attributed to the antisymmetric stretching of $PO_4$.[40] These results indicate that $Ca3(PO_4)_2$ molecules were attached to the surface of Cur@NaCas NPs by co-precipitation to form the external CaP shell.

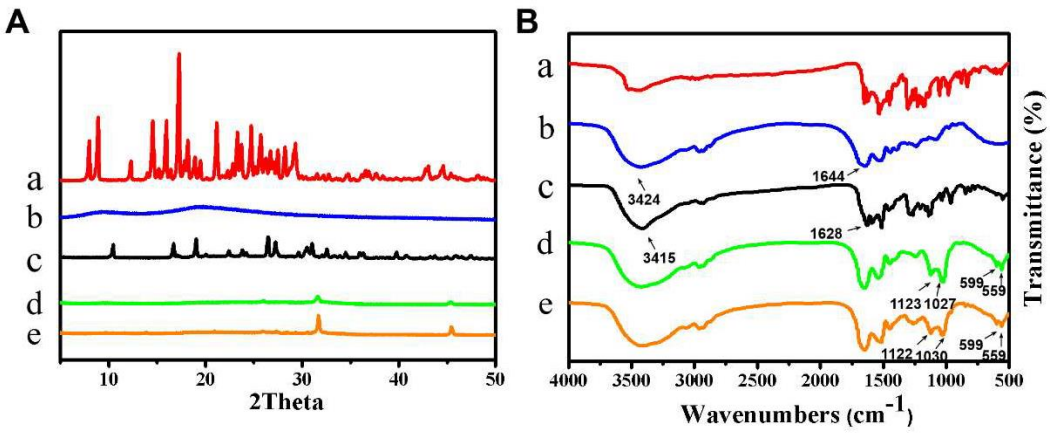


**Figure 2.** (A) X-ray diffraction patterns and (B) Fourier-transform infrared spectra of the Cur (a), NaCas (b), Cur@NaCas NPs (c), (Cur@NaCas)@CaP NPs (d) and NaCas@CaP NPs (e).

Zeta-potential was also used to confirm the loading of Cur and the formation of core-shell structure **(Figure 3A).** The zeta-potential values of NaCas decreased from -22.1 to -32.5 after self-assembly with Cur, indicating an enhanced anionic surface coating on Cur@NaCas. When loading Cur in proteins, NaCas reassembled to lower

301 the number of less negatively charged K-casem and raise the number of high
302 negatively charged casein (asl -, as2-, -), which increased the overall magnitude of
303 the negative zeta-potential.[41] The zeta potential of CaP was -16.4 mV, which
304 represents the anionic nature of CaP. Following entrapment of Cur@CaNas by
305 $Ca3(PO_4)_2$, the zeta-potential of NPs was marginally increased to -15.7 mV. This
306 confirmed that the shielding by a CaP layer on the surface of Cur@NaCas altered the
307 negative charge.[42] This higher zeta-potential of (Cur@NaCas)@CaP NPs would be
308 beneficial for its uptake into cells compared with NaCas NPs because of the lower
309 electrostatic repulsion, relative to the negatively charged surfaces of cancer cells,
310 which lowers the barrier to diffuse into cells.[43, 44] This hypothesis has been further
311 investigated in subsequent experiments.

312 Fluorescence spectrum was applied to study the intrinsic fluorescence of Cur as
313 the microenvironment changes in aqueous systems **(Figure 3B).** At an excitation
314 wavelength of 420 nm, Cur dissolved in ethanol showed the maximum light intensity
315 at 535 nm, while Cur dispersed in water almost without fluorescence. The blue shift
316 of Cur peak at 535 nm, to 517 nm after encapsulation of NaCas NPs, and the
317 fluorescence intensity increased at the same time. It explained that Cur was loaded
318 into the core of NaCas by hydrophobic interactions, which provided hydrophobic
319 regions for Cur.[45] After the CaP coating, the blue shift of Cur peak from 517 nm to
320 506.2 nm, and the further increased fluorescence intensity indicated that the surface of
321 NaCas was coated by CaP to form a more hydrophobic matrix.

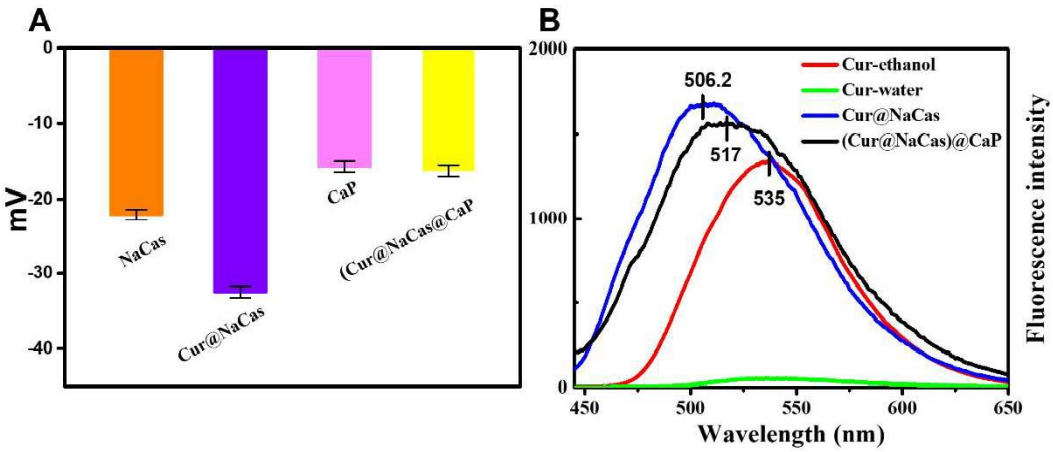


**Figure 3.** (A) Average zeta-potential ofNPs. (B) Fluorescence emission spectra of Cur and NPs.

### 3.2 Thermal and UV Stability of (Cur@NaCas)@CaP

Thermal instability in aqueous solution is a major factor that limits Cur bioavailability.[46] This can be further confirmed in our experiment **(Figure 4A).** The rest of free Cur was 10.53 % after stored at 80 °C for 120 min, while 72.9 % of Cur remaining at 25 °C. It was also found that NaCas encapsulation only limitedly improved the thermal stability of Cur. After encapsulated with CaP coating, the remaining Cur dramatically reached at 81.54 % under the same heating treatment. Then, we studied the degradation kinetics of free and encapsulated Cur in aqueous solution. Both free and NaCas encapsulated Cur displayed significantly faster degradation at 80 °C than 25 °C **(Figure 4B and Figure Sl ).** After heated for 5 min at 80 °C, more than 60 % of free Cur was lost. However, more than 99 % of Cur loaded in the NaCas@CaP NPs remained. When the heating time reached to 45 min, NaCas loaded Cur showed about 50 % of loss. In contrast, about 90 % of the NaCas@CaP

loaded Cur remained. After heated for 120 min at 80 °C, the aqueous solution of free and NaCas loaded Cur became transparent, and their colors faded (Seen the insert photos in **Figure 4B).** As reported, about 50 % of soy protein isolate loaded Cur was inactivated at 95 °C within 30 mins,[12] while the Cur encapsulated by NaCas@CaP NPs didn't show sharp reduction within 2 h under high thermal condition. Thus, the above results indicated that CaP surface coating could efficiently protect the guest molecules from the thermal degradation.

Cur also easily degraded under UV-light.[47] Stored in the UV-light conditions **(Figure 4C),** free Cur had a sharp degraded by about 81.75 % after storage of 30 min and more than 90 % of free Cur degraded in 120 min. For NaCas NPs, almost 43 % of loaded Cur degraded after 120 min. With CaP coating on the surface of NaCas, there was a partial degradation by 12 % in 30 min, and then maintained a certainly stability. Obviously, the shell of CaP provided a superior UV protection of at least 1.4 folds than NaCas, and 8 folds better than free Cur.

### 3.3 pH-Responsive Release Comparison of Cur from NaCas with or without CaP Coating

In practical applications the intend is not to retain the encapsulated compound indefinitely. Instead, the intend would be to facilitate protection of the encapsulated compounds prior to reaching its target, but then have a slow and regular release to limit the rate of physical applications. In this work, the *in vitro* release experiments of Cur@NaCas NPs and (Cur@NaCas)@CaP NPs in different PBS buffer (pH 7.4 and

5.5) were investigated and shown in **Figure** 4D. The whole release procedure lasted 12 h, and Tween 80 (1% w/v) was added to enhance the stability of Cur.[48] At both 7.4 and 5.5, more than 95 % of Cur loaded in NaCas NPs was released within 4 h. Thus, a single protein carrier consisting of NaCas has the capability of facilitating a pH-response release, however, the relative fast release could cause substantial drug leakage and inactivation. Previous studies have shown that CaP is also a pH-sensitive material.[31, 49] When encapsulated in a NaCas@CaP hybrid matrix, only 30 % of Cur was released at 4 h in physiological pH (pH 7.4), while 66.9 % of Cur was released after 12 h at pH 7.4. By contrast, the cumulative release of Cur reached to 99.8 % after 12 h at pH 5.5 (Figure 4D). Therefore, the pH-responsive release behavior of NaCas@CaP NPs retards the premature drug release and subsequent rapid degradation/deactivation of the drugs after administration, and achieves controlled release around the acidic microenvironments of tumors sites.[48, 50]

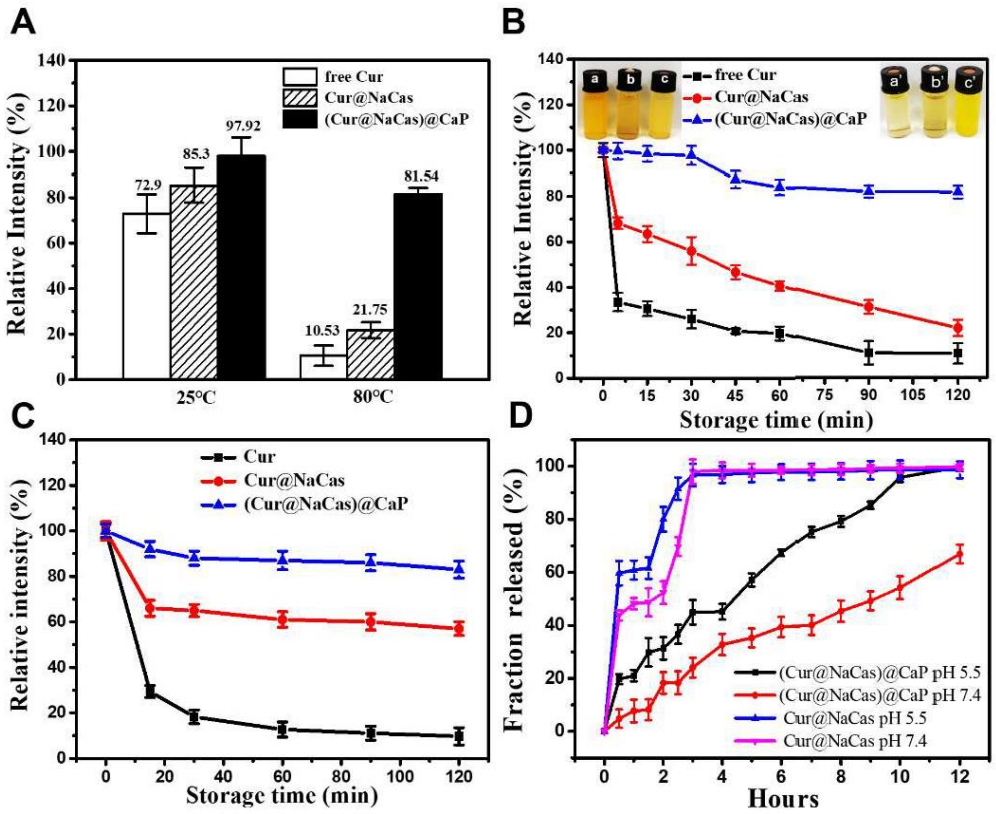


**Figure 4.** (A) In vitro stability of free Cur and Cur in the nanoparticles in water at pH 7.4 upon storage in 120 min at 25 °C and 80 °C.(B) Degradation kinetics of free Cur and Cur in the NPs in water at 80 °C from up to 120 min , and the changes of free Cur(a and a') , Cur@NaCas (band b') and (Cur@NaCas)@CaP (c and c' ) before and after heating were shown in the picture.(C) Degradation kinetics of free Cur and Cur in the NPs under ultraviolet light at 25 °C.(D) Release profiles of Cur@NaCas NPs and (Cur@NaCas)@CaP NPs at PBS (pH 7.4 and 5.5) in 12 h.

### 3.4 Improved Cellular Uptake ofNaCas@CaP loaded Cur

Confocal laser scanning microscopy (CLSM) was used to investigate whether encapsulated compounds have improved cellular uptake capacity. The CLSM images through the A549 monolayer cells after incubation with DMSO, free Cur,

Cur@NaCas NPs, and (Cur@NaCas)@CaP NPs (all with equivalent concentration of Cur) are shown in in **Figure 5.** The commercial fluorescent dye propidium iodide (PI) was used to characterize cell morphology, and the fluorescence of Cur indicates the cell uptake of NPs. (Cur@NaCas)@CaP NPs showed stronger green fluorescent intensity than an equal concentration of free Cur and NaCas loaded Cur, suggesting NaCas@CaP NPs can improve the cellular uptake ability of encapsulated hydrophobic compounds. The reason for the lower green fluorescent intensity for the Cur@NaCas NPs might be due to leakage of Cur from Cur@NaCas NPs. Free Cur was shown to degrade rapidly and as such reduce its bioavailability at a slightly acidic cancer cell environment pH **(Figure S2).** For the (Cur@NaCas)@CaP NPs, the presence of a CaP shell increased the stability of Cur in a physiological aqueous environment and reduced the cell uptake barriers between NPs and Cur (Figure 5), thus evidencing improved cellular uptake and stability.[51 , 52] On the other hand, Cur would be released from the NaCas core of the (Cur@NaCas)@CaP NPs following cellular uptake. It is likely that any intracellular release would have been in part facilitated by endosomes and lysosomes, and achieved a cumulative intracellular release.[53] Thus, the synergistic effect of shell and core increased the cell uptake capacity of NPs and achieved efficient intracellular release.

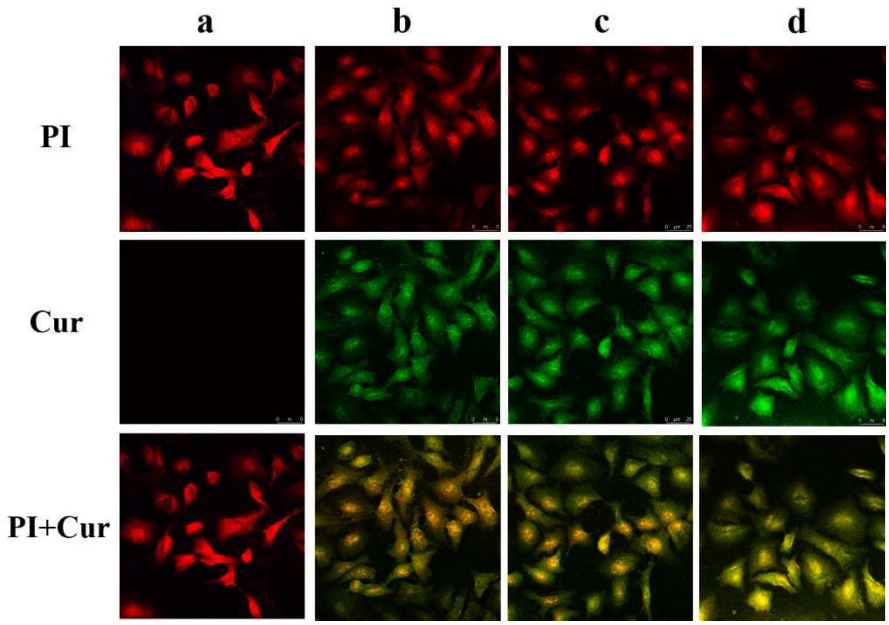


**Figure 5.** Uptake of free Cur and encapsulated Cur into epithelial cells (A549, human alveolar basal epithelial cells) as observed by confocal laser scanning microscopy (CLSM) afte 4h of exposure. Column ' PI' , Propidium iodide (PI)-only control; Column ' Cur', Cur-only control; Column ' PI + Cur' , cells treated with both PI and Cur. (a) cells treated with DMSO; (b) cells treated with free Cur; (c) cells treated with Cur@NaCas NPs; and (d) cells treated with (Cur@NaCas)@CaP NPs

### 3.5 Cellular Antioxidant Activity

It has previously been shown that Cur has antioxidant activity and free radical scavenging activities.[47] The cellular anti-oxidant activity (CAA) of free Cur and encapsulated Cur were assessed by the MGC-803 cell model **(Figure** 6A), and the anti-proliferation activities of NPs on MGC-803 cells are shown in **Figure S3.** According to the principle of CAA, peroxy radicals produced by ABAP cause oxidation of DCFH to form the fluorescent DCF, the DCF fluorescence intensity reflects the degree of oxidation damage caused by free radicals.[35] The antioxidant

capacity of any natural compounds can be reflected by the reduced DCF fluorescence intensity. The results **(Figure** 6A) indicated that DCF accumulated continuously in the cells over time, while Cur could quench free radicals to reduce the concentration of intracellular DCF. The reduced accumulation of DCF demonstrates that both the added Cur@NaCas NPs and (Cur@NaCas)@CaP NPs have antioxidant activity, which is consistent with previous work that reported that Cur loaded inclusion complexes possessed a higher free radical scavenging capacity compared with free Cur.[54] The CAA value were determined using eq.(3). The CAA results indicate that the NaCas and NaCas@CaP NPs loaded Cur had better cellular anti-oxidant activity than free Cur **(Figure** 6B).

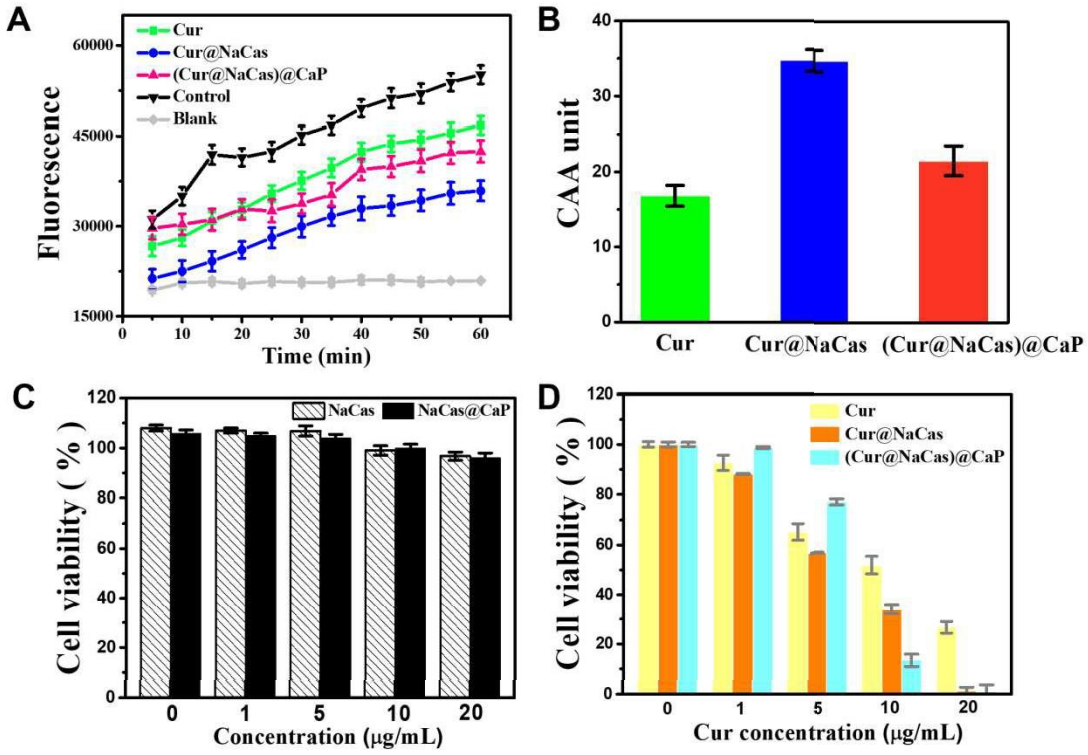


**Figure 6.** (A) The kinetics curve of DCF fluorescence from cellular anti-oxidant activity (CAA) of Cur, Cur@NaCas, (Cur@NaCas)@CaP, control, and blank sample.

In all instances the cells were exposed to equal amount of Cur. Error bars indicate the standard deviation following triplicate determinations. (B)The comparison of cellular anti-oxidant activity value for different samples. (C) Anti-proliferation activity the blank NPs toxicity of human alveolar basal epithelial cells (A549 cells). (D) Anti-proliferation activity of 1, 5, 10 and 20 μg/mL DMSO-dissolved and encapsulated Cur against A549 cells.

### 3.6 Cell Viability

In order to investigate the cytotoxicity of (Cur@NaCas)@CaP NPs in cancer cells, we monitored the cell proliferation using human alveolar basal epithelial cancer cells (A549 cells) as a model. The native NaCas and NaCas@CaP NPs (without Cur) showed almost 100 % cell viability at 72 h **(Figure** 6C), indicating that the blank nanoparticle was nontoxic and biocompatible with the cell model used in these experiments.[55] However, with Cur encapsulated in either NaCas or NaCas@CaP NPs showed an improved anti-proliferation activity against A549 cancer cells when compared with free Cur **(Figure** 6D). When the concentration of free Cur was applied at 1 μg/mL and 5 μg/mL, it showed a mean cell viability of 92.6 % and 65.2 % respectively; while the Cur@NaCas inclusion complex showed a mean cell viability of 88.2 % and 56.6 % at 1 μg/mL and 5 μg/mL of free Cur equivalent respectively. The (Cur@NaCas)@CaP inclusion complex did not show the same enhanced anti-proliferation effect on A549 cells compared to free Cur at the same Cur concentration, with a mean cell viability of 98.8 % and 77.0 % at 1 μg/mL and 5 μg/mL of free Cur

equivalent respectively. A more prominent improvement in the anti-proliferation activity of NaCas@CaP loaded Cur was observed at an effective dose of free Cur 10 µg/mL, with a mean cell viability of 13.5 %. At the same effective Cur concentration, the cell viability of free Cur and Cur@NaCas NPs was 51.7 % and 34.0 %. It appears that the anticancer effect of NPs loaded with Cur was related to the release property and biocompatibility of NPs, which is also relevant to the instability, insolubility and concentration of Cur.[42, 56] More specifically, when considering Cur at a lower concentration, the release rate of Cur from the NPs was less than the rate of deg radation, which resulted in a lower anti-cancer activity of the encapsulated Cur compared to free Cur. At the higher concentration, free Cur gradually degraded in aqueous conditions in which the experiments were carried out, due to Cur' s instability and low biocompatibility; This while the chemical stability of NPs loaded Cur at the same equivalent concentrations was remarkably enhanced (Figure 6D). It appears that the NaCas@CaP loaded Cur achieved a more continuous anti-cancer effect, which agrees with the CLSM results in this research (Figure 5). At the highest concentration tested (20 µg/mL) in this study, the cell viability of A549 cells exposed to both Cur@NaCas loaded and (Cur@NaCas)@CaP loaded NPs was almost non-existent, while the addition of an equivalent concertation of free Cur saw a viability of approximately 30%. This could be ascribed to the degradation of free Cur under the experimental conditions where some of the added free Cur might have already degraded before its full weight of the higher concentration could affect the cells

(Figure S2), plus, it might have been possible that the higher concentration saturated the anti-proliferation effect against A549 cancer cells.

## 4. Conclusions

In conclusion, a novel hybrid nanodelivery system was prepared using NaCas and CaP. The nanosized NaCas@CaP NPs were shown to have an obvious core-shell structure, which markedly improved the stability of Cur under thermal conditions and UV light conditions. Besides, the pH-responsive release of Cur around cancer cell environment was achieved. Furthermore, the results proved that NaCas@CaP NPs can improve anti-oxidant activity, cell uptake ability and anti-proliferative activity of Cur in living cells. Our research provided a simple and stable nano-platform for encapsulating sensitive hydrophobic biomolecules. The results revealed that this core-shell nanodelivery system was meaningful for keeping bioactivities of sensitive molecules and improving the bioavailability in cancer treatment. Thus, this nanodelivery system is expected to be applied for in food and pharmaceutical products field.

For human health and practical application , further research is still undergoing in our laboratory including the delivery behavior and uptake mechanism of this nanodelivery system in various food and animals' systems, as well as the bioactivities of encapsulated molecules after the delivery of gastrointestinal tract.

AUTHOR INFORMATION

## Author Contributions

The first two authors have equal contributions

## Notes

The authors declare no competing financial interest.

## ACKNOWLEDGMENT

The authors acknowledged financial support from the National Natural Science Foundation of China (21878014), the Double First-rate Program (ylkxj03), and the 111 Project (B13005).

## REFERENCES

[1] X. Duan, H. Chen, L. Fan, J. Kong, Drug Self-Assembled Delivery System with Dual Responsiveness for Cancer Chemotherapy, ACS Biomater Sci Eng 2(12) (2016) 2347-2354.
[2] Y. Li, Y. Wang, G. Huang, J. Gao, Cooperativity Principles in Self-Assembled Nanomedicine , Chem Rev 118(11) (2018) 5359-5391.
[3] W. Cui, J. Li, G. Decher, Self-Assembled Smart Nanocarriers for Targeted Drug Delivery, Adv Mater 28(6) (2016) 1302-11.
[4] M.H. Li, Z. Luo, Y.L. Zhao, Self-Assembled Hybrid Nanostructures: Versatile Multifunctional Nanoplatforms for Cancer Diagnosis and Therapy, Chem Mater 30(1) (2018) 25-53.
[5] L. Zhou, T. Qiu, F. Lv, L. Liu, J. Ying, S. Wang, Self-Assembled Nanomedicines for Anticancer and Antibacterial Applications, Adv Healthc Mater 7(20) (2018) e1800670.
[6] Y.M.a.H. Maeda, A New Concept for Macromolecular Therapeutics in Cancer Chemotherapy: Mechanism of Tumoritropic Accumulation of Proteins and the Antitumor Agent Smancsl, Cancer Res 46 (1986) 6387-6392.
[7] Y. Jin, R. Xin, P. Ai, D. Chen, Self-assembled drug delivery systems 2. Cholesteryl derivatives of antiviral nucleoside analogues: synthesis, properties and the vesicle formation, Int J Pharm 350(1-2) (2008) 330-7.
[8] D. Kalyane, N. Raval, R. Maheshwari, V. Tambe, K. Kalia, R.K. Tekade, Employment of enhanced permeability and retention effect (EPR): Nanoparticle-based precision tools for targeting of therapeutic and diagnostic agent in cancer, Mater Sci Eng C 98 (2019) 1252-1276.

[9] S.Y. Qin, A.Q. Zhang, S.X. Cheng, L. Rong, X.Z. Zhang, Drug self-delivery systems for cancer therapy, Biomaterials 112 (2017) 234-247.
[1O] S. Jaiswal, P. Mishra, Co-delivery of curcumin and serratiopeptidase in HeLa and MCF-7 cells through nanoparticles show improved anti-cancer activity, Mater Sci Eng C 92 (2018) 673-684.
[11] H. Lu, Q. Wang, G. Li, Y. Qiu, Q. Wei, Electrospun water-stable zein/ethyl cellulose composite nanofiber and its drug release properties, Mater Sci Eng C 74 (2017) 86-93.
[12] F.P. Chen, B.S. Li, C.H. Tang, Nanocomplexation between curcumin and soy protein isolate: influence on curcumin stability/bioaccessibility and in vitro protein digestibility, J Agric Food Chem 63(13) (2015) 3559-69.
[13] W. Kajthunyakarn, D. Sakloetsakun, T. Pongjanyakul, Sodium caseinate-magnesium aluminum silicate nanocomposite films for modified-release tablets, Mater Sci Eng C 92 (2018) 827-839.
[14] R. Li, Y. Ma, Y. Dong, Z. Zhao, C. You, S. Huang, X. Li, F. Wang, Y. Zhang, Novel Paclitaxel-Loaded Nanoparticles Based on Human H Chain Ferritin for Tumor-Targeted Delivery, ACS Biomater Sci Eng 5 (2019) 6645-6654.
[15] K. Pan, H. Chen, S.J. Baek, Q. Zhong, Self-assembled curcumin-soluble soybean polysaccharide nanoparticles: Physicochemical properties and in vitro anti-proliferation activity against cancer cells, Food Chem 246 (2018) 82-89.
[16] Y. Zhang, Q.X. Zhong, Encapsulation of bixin in sodium caseinate to deliver the colorant in transparent dispersions, Food Hydrocoll 33(1) (2013) 1-9.
[17] 0. Menendez-Aguirre, A. Kessler, W. Stuetz, T. Grune, J. Weiss, J. Hinrichs, Increased loading of vitamin D2 in reassembled casein micelles with temperature-modulated high pressure treatment, Food Res Int 64 (2014) 74-80.
[18] R. Penalva, I. Esparza, M. Agueros, C.J. Gonzalez-Navarro, C. Gonzalez-Ferrero, J.M. Irache, Casein nanoparticles as carriers for the oral delivery of folic acid, Food Hydrocoll 44 (2015) 399-406.
[19] A. Rashidinejad, S.M. Loveday, G.B. Jameson, J.P. Hindmarsh, H. Singh, Rutin-casein co-precipitates as potential delivery vehicles for flavonoid rutin, Food Hydrocoll 96 (2019) 451-462.
[20] A. Bahri, M. Martin, C. Gergely, S. Marchesseau, D. Chevalier-Lucia, Topographical and nanomechanical characterization of casein nanogel particles using atomic force microscopy, Food Hydrocoll 83 (2018) 53-60.
[21] C. Moitzi, I. Portnaya, 0. Glatter, 0. Ramon, D. Danino, Effect of Temperature on Self-Assembly of Bovine -Casein above and below Isoelectric pH. Structural Analysis by Cryogenic-Transmission Electron Microscopy and Small-Angle X-ray Scattering, Langmuir 24(7) (2008) 3020-3029.
[22] M. Li, M.A.E. Auty, S.V. Crowley, A.L. Kelly, J.A. O'Mahony, A. Brodkorb, Self-association of bovine -casein as influenced by calcium chloride, buffer type and temperature, Food Hydrocoll 88 (2019) 190-198.
[23] Y. Luo, K. Pan, Q. Zhong, Casein/pectin nanocomplexes as potential oral delivery vehicles, Int J Pharm 486(1-2) (2015) 59-68.
[24] Q. Hu, M. Bae, E. Fleming, J.-Y. Lee, Y. Luo, Biocompatible polymeric

nanoparticles with exceptional gastrointestinal stability as oral delivery vehicles for lipophilic bioactives, Food Hydrocoll, 89 (2019) 386-395..
[25] C. Sun, Y. Gao, Q. Zhong, Properties of Ternary Biopolymer Nanocomplexes of Zein, Sodium Caseinate, and Propylene Glycol Alginate and Their Functions of Stabilizing High Internal Phase Pickering Emulsions, Langmuir 34(31) (2018) 9215-9227.
[26] H. Zhang, Y. Fu, Y. Xu, F. Niu, Z. Li, C. Ba, B. Jin, G. Chen, X. Li, One-step assembly of zein/caseinate/alginate nanoparticles for encapsulation and improved bioaccessibility of propolis, Food Funct 10(2) (2019) 635-645.
[27] M. Yerramilli, S. Ghosh, Long-term stability of sodium caseinate-stabilized nanoemulsions, **J** Food Sci Technol 54(1) (2017) 82-92.
[28] Q. Hu, M. Bae, E. Fleming, J.-Y. Lee, Y. Luo, Biocompatible polymeric nanoparticles with exceptional gastrointestinal stability as oral delivery vehicles for lipophilic bioactives, Food Hydrocoll 89 (2019) 386-395.
[29] H.B. Yao, M.R. Gao, S.H. Yu, Small organic molecule templating synthesis of organic-inorganic hybrid materials: their nanostructures and properties, Nanoscale 2(3) (2010) 323-34.
[30] E. Soo, S. Thakur, Z. Qu, S. Jambhrunkar, H.S. Parekh, A. Popat, Enhancing delivery and cytotoxicity of resveratrol through a dual nanoencapsulation approach, **J** Colloid Interface Sci 462 (2016) 368-74.
[31] P. Mi, D. Kokuryo, H. Cabral, H. Wu, Y. Terada, T. Saga, I. Aoki, N. Nishiyama, K. Kataoka, A pH-activatable nanoparticle with signal-amplification capabilities for non-invasive imaging of tumour malignancy, Nat Nanotechnol 11(8) (2016) 724-30.
[32] F. Li, Q. Xing, Y. Han, Y. Li, W. Wang, T.S.H. Perera, H. Dai, Ultrasonically assisted preparation of poly(acrylic acid)/calcium phosphate hybrid nanogels as pH-responsive drug carriers, Mater Sci Eng C 80 (2017) 688-697.
[33] Q. Song, L. Li, K. Xiong, W. Tian, J. Lu, J. Wang, N. Huang, Q. Tu, Z. Yang, A facile dopamine-mediated metal-catecholamine coating for therapeutic nitric oxide gas interface-catalytic engineering of vascular devices, Biomater Sci 7(9) (2019) 3741-3750.
[34] M. Canillas, P. Pena, A.H. de Aza, M.A. Rodriguez, Calcium phosphates for biomedical applications, Boletin de la Sociedad Espanola de Ceramica y Vidrio 56(3) (2017) 91-112.
[35] Z. Liu, Q. Wu, **J.** He, F. Vriesekoop, H. Liang, Crystal-Seeded Growth of pH-Responsive Metal-Organic Frameworks for Enhancing Encapsulation, Stability, and Bioactivity of Hydrophobicity Compounds, ACS Biomater Sci Eng 5 (2019) 6581-6589.
[36] A.F. Martins, P.V. Bueno, E.A. Almeida, F.H. Rodrigues, A.F. Rubira, E.C. Muniz, Characterization of N-trimethyl chitosan/alginate complexes and curcurnin release, Int **J** Biol Macromol 57 (2013) 174-84.
[37] J. Wu, **J.** Wang, J. Zhang, Z. Zheng, D.L. Kaplan, G. Li, X. Wang, Oral Delivery of Curcumin Using Silk Nano- and Microparticles, ACS Biomater Sci Eng 4(11) (2018) 3885-3894.

[38] H. Xiang, D. Sun-Waterhouse, C. Cui, W. Wang, K. Dong, Modification of soy protein isolate by glutaminase for nanocomplexation with curcumin, Food Chem 268 (2018) 504-512.
[39] H.Q. Chen, Q.X. Zhong, Processes improving the dispersibility of spray-dried zein nanoparticles using sodium caseinate, Food Hydrocoll 35 (2014) 358-366.
[40] W.-H. Lee, C.-Y. Loo, R. Rohanizadeh, Functionalizing the surface of hydroxyapatite drug carrier with carboxylic acid groups to modulate the loading and release of curcumin nanoparticles, Mater Sci Eng C 99 (2019) 929-939.
[41] K. Pan, H. Chen, P.M. Davidson, Q. Zhong, Thymol nanoencapsulated by sodium caseinate: physical and antilisterial properties, J Agric Food Chem 62(7) (2014) 1649-57.
[42] B. Deng, M. Xia, J. Qian, R. Li, L. Li, J. Shen, G. Li, Y. Xie, Calcium Phosphate-Reinforced Reduction-Sensitive Hyaluronic Acid Micelles for Delivering Paclitaxel in Cancer Therapy, Mol Pharm 14(6) (2017) 1938-1949.
[43] A. Verma, F. Stellacci, Effect of Surface Properties on Nanoparticle-Cell Interactions, Small 6(1) (2010) 12-21.
[44] Z. Zhou, Y. Shen, J. Tang, E. Jin, X. Ma, Q. Sun, B. Zhang, E.A. Van Kirk, W.J. Murdoch, Linear polyethyleneimine-based charge-reversal nanoparticles for nuclear-targeted drug delivery, J Mater Chem 21(47) (2011) 19114-19123.
[45] K. Pan, Q. Zhong, S.J. Baek, Enhanced dispersibility and bioactivity of curcumin by encapsulation in casein nanocapsules, J Agric Food Chem 61(25) (2013) 6036-43.
[46] M. Kharat, Z. Du, G. Zhang, D.J. McClements, Physical and Chemical Stability of Curcumin in Aqueous Solutions and Emulsions: Impact of pH, Temperature, and Molecular Environment, J Agric Food Chem 65(8) (2017) 1525-1532.
[47] Z. Hussain, H.E. Thu, M.W. Amjad, F. Hussain, T.A. Ahmed, S. Khan, Exploring recent developments to improve antioxidant, anti-inflammatory and antimicrobial efficacy of curcumin: A review of new trends and future perspectives, Mater Sci Eng C 77 (2017) 1316-1326.
[48] M. Zheng, S. Liu, X. Guan, Z. Xie, One-Step Synthesis of Nanoscale Zeolitic Imidazolate Frameworks with High Curcumin Loading for Treatment of Cervical Cancer, ACS Appl Mater Interfaces 7(40) (2015) 22181-7.
[49] P. Mi, N. Dewi, H. Yanagie, D. Kokuryo, M. Suzuki, Y. Sakurai, Y. Li, I. Aoki, K. Ono, H. Takahashi, H. Cabral, N. Nishiyama, K. Kataoka, Hybrid Calcium Phosphate-Polymeric Micelles Incorporating Gadolinium Chelates for Imaging-Guided Gadolinium Neutron Capture Tumor Therapy, ACS Nano 9(6) (2015) 5913-5921.
[50] L. Liu, J. Guo, P. Liu, Raspberry-Shaped Independent Temperature and pH Dual-Responsive CPMAA@CPNIPAM Yolk/Shell Microspheres for Site-Specific Targeted Delivery of Anticancer Drugs, Ind Eng Chem Res 55(16) (2016) 4790-4796.
[51] Y. Luo, Z. Teng, T.T. Wang, Q. Wang, Cellular uptake and transport of zein nanoparticles: effects of sodium caseinate, J Agric Food Chem 61(31) (2013) 7621-9.
[52] P. Das, N.R. Jana, Length-Controlled Synthesis of Calcium Phosphate Nanorod and Nanowire and Application in Intracellular Protein Delivery, ACS Appl Mater Interfaces 8(13) (2016) 8710-20.

[53] S.J. Kaczmarczyk, K. Sitaraman, H.A. Young, S.H. Hughes, D.K. Chatterjee, Protein delivery using engineered virus-like particles, Proc Natl Acad Sci U S A 108(41) (2011) 16998-7003.
[54] P. Jiang, J. Huang, C. Bao, L. Jiao, H. Zhao, Y. Du, F. Ren, Y. Li, Enzymatically partial hydrolyzed a-lactalbumin peptides for self-assembled micelles formation and their application for coencapsulation of multiple anti-oxidants, J Agric Food Chem 66 (2018) 12921-12930.
[55] W.H. Lee, C.Y. Loo, R. Rohanizadeh, Functionalizing the surface of hydroxyapatite drug carrier with carboxylic acid groups to modulate the loading and release of curcumin nanoparticles, Mater Sci Eng C 99 (2019) 929-939.
[56] B. Lei, M. Wang, Z. Jiang, W. Qi, R. Su, Z. He, Constructing Redox-Responsive Metal-Organic Framework Nanocarriers for Anticancer Drug Delivery, ACS Appl Mater Interfaces 10(19) (2018) 16698-16706.

**Declaration of interests**

D The authors declare that they have no known competing financial interests or personal relationships that could have appeared to influence the work reported in this paper.

☐The authors declare the following financial interests/personal relationships which may be considered as potential competing interests:

# Author Statement

Hao Liang:

Conceptualization, methodology, resources, project administration,lwriting - original draft, writing - review & editing, supervision, funding acquisition

Qiao Wu:

Conceptualization, methodology, validation, formal analysis, investigation, data curation, writing - original draft

Huiling Gao

Conceptualization, methodology, supervision

Frank Vriesekoop

Formal analysis, writing - original draft, writing - review & editing

Zexun Liu

Methodology, resources.

Jie He

Methodology

# Supporting Information

## Calcium Phosphate Coated Core-Shell Protein Nanocarriers: Robust Stability, Controlled Release and Enhanced Anticancer Activity for Curcumin Delivery

Qiao Wu[a] Huiling Gao[a] Frank Vriesekoop[c] Zexun Liu[a] Jie He[a] Hao Liang*[a b]

[a] State Key Laboratory of Chemical Resource Engineering, Beijing University of Chemical Technology, Beijing100029, P.R. China

[b] Qinhuangdao Bohai Biological Research Institute of Beijing University of Chemical Technology, Qinhuangdao 066000, China

[c] Department of Food Technology and Innovation, Harper Adams University, Newport TFl0 8NB, Shropshire, United Kingdom.

Corresponding Author

* E-mail: lianghao@rnail.buct.edu.cn

## Supplementary tables

**Table S1 Effect of NaCas concentration on drug loading efficiency (DLE)** (%).

| NaCas (mg/mL) | Cur (mg/mL) | Stirring speed (rpm/min) | Stirring time (h) | DLE (%) |
|---|---|---|---|---|
| 0.5 | 0.5 | 600 | 1.5 | 62.34±1.30 |
| 0.75 | 0.5 | 600 | 1.5 | 78.67±1.14 |
| **1** | 0.5 | 600 | 1.5 | 80.63±1.37 |
| 1.25 | 0.5 | 600 | 1.5 | 80.94±1.43 |
| 1.5 | 0.5 | 600 | 1.5 | 81.13±1.29 |

All samples were prepared at room temperature.

**Table S2 Effect of stirring speed on DLE** (%)

| NaCas (mg/mL) | Cur (mg/mL) | Stirring speed (rpm/min) | Stirring time (h) | DLE (%) |
|---|---|---|---|---|
| **1** | 0.5 | 400 | 1.5 | 57.83±1.17 |
| **1** | 0.5 | 500 | 1.5 | 63.49±1.23 |
| **1** | 0.5 | 600 | 1.5 | 80.98±1.27 |
| **1** | 0.5 | 700 | 1.5 | 84.24±1.31 |
| **1** | 0.5 | 800 | 1.5 | 84.32±1.43 |

All samples were prepared at room temperature.

**Table S3 Effect of stirring time on DLE** (%)

| NaCas (mg/mL) | Cur (mg/mL) | Stirring speed (rpm/min) | Stirring time (h) | DLE (%) |
|---|---|---|---|---|
| **1** | 0.5 | 700 | 0.5 | 50.64±1.34 |
| **1** | 0.5 | 700 | 1.0 | 73.68±1.49 |
| **1** | 0.5 | 700 | 1.5 | 84.97±1.38 |
| **1** | 0.5 | 700 | 2.0 | 90.01±1.29 |
| **1** | 0.5 | 700 | 2.5 | 90.27±1.44 |

All samples were prepared at room temperature.

**Table S4 Effect of the added CaP volume on DLE** (%)

| CaP concentration (mM) | CaP volume (μL) | Mixing time (min) | DLE (%) |
|---|---|---|---|
| 50 | 5 | 2 | 21.57±2.06 |
| 50 | 10 | 2 | 53.24±1.92 |
| 50 | 15 | 2 | 80.42±2.14 |
| 50 | 20 | 2 | 99.25±1.97 |
| 50 | 25 | 2 | 99.47±2.03 |

All samples were prepared at room temperature.

Supplementary figures

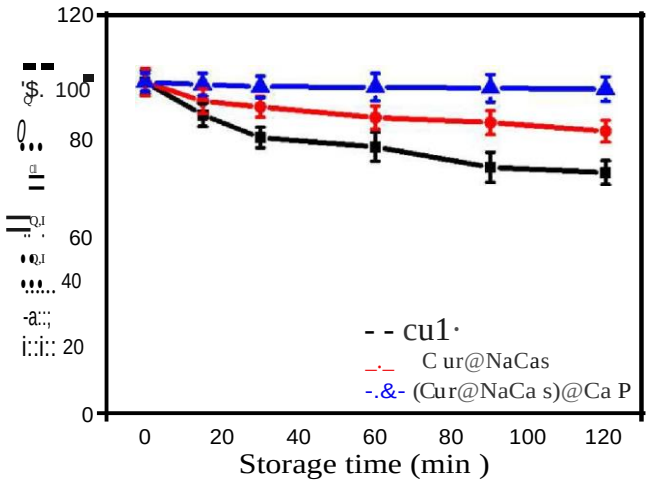


Figure S1 Degradation kinetics of free Cur and Cur in the NPs in water from up to120 min at 25 °C.

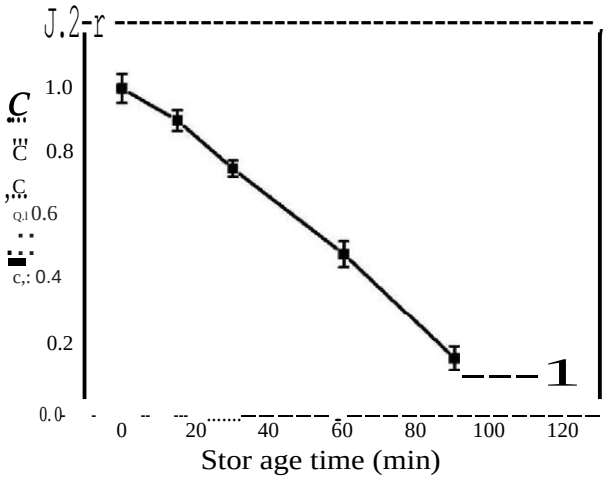


Figure S2 Degradation kinetics of free Cur at pH 5.5 PBS.

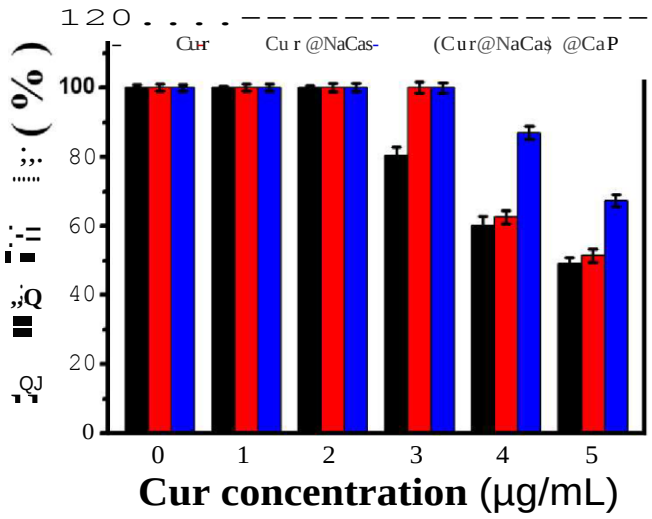


Figure S3 Anti-proliferation activity of 1, 2, 3, 4 and 5 μg/mL DMSO-dissolved and encapsulated Cur against MGC-803 cells, and treatment for 24 h.